Copy 216

[redacted]

RM A56C06

[redacted]

Reg # 18947

3 JUL 1956

NACA

TECHNICAL LIBRARY
AFL 2811

TECH LIBRARY KAFB, NM
0143511

NACA RM A56C06

6489

RESEARCH MEMORANDUM

THE CHANGE WITH MASS-FLOW RATIO OF THE COWL PRESSURE DRAG OF NORMAL-SHOCK INLETS AT SUPERSONIC SPEEDS

By Wallace F. Davis and Forrest E. Gowen

Ames Aeronautical Laboratory
Moffett Field, Calif.

Classification Cancelled (Unclassified)

By authority of NASA Tech Pub Announcement #8
(OFFICER AUTHORIZED TO CHANGE)

By ..... 26 Aug 59
NAME AND

..... NK .....
GRADE OF OFFICER MAKING CHANGE)

9 Mar 61
DATE

CLASSIFIED DOCUMENT

This material contains information affecting the National Defense of the United States within the meaning of the espionage laws, Title 18, U.S.C., Secs. 793 and 794, the transmission or revelation of which in any manner to an unauthorized person is prohibited by law.

NATIONAL ADVISORY COMMITTEE FOR AERONAUTICS

WASHINGTON

June 22, 1956

[redacted]

TECH LIBRARY KAFB, NM
0143511

NATIONAL ADVISORY COMMITTEE FOR AERONAUTICS

RESEARCH MEMORANDUM

THE CHANGE WITH MASS-FLOW RATIO OF THE COWL PRESSURE DRAG OF NORMAL-SHOCK INLETS AT SUPERSONIC SPEEDS

By Wallace F. Davis and Forrest E. Gowen

SUMMARY

Pressure-drag coefficients and the changes in these coefficients with mass-flow ratio have been measured in tests of six open-nose conical cowls at an angle of attack of 0°. The tests were performed in the Ames 8- by 8-inch supersonic wind tunnel at Mach numbers from 1.3 to 1.9 and at a Reynolds number, based on the model reference diameter, of about 2.4 million. The models had cowl angles of 5°, 10°, and 15°, and the 5° cowl was tested with four lip shapes - from a sharp to a relatively blunt leading edge.

The results of the tests show that, for cowl angles less than about 5°, the method of Fraenkel, which does not account for lip shape (R.A.E. TN 2380, 1950), is adequate for predicting the decrease in cowl pressure drag with a reduction in mass-flow ratio from 1.0 to about 0.8. For such slender cowls, the magnitude of this drag reduction decreases with flight Mach number so that it becomes insignificant at Mach numbers greater than about 2. For cowl angles of 10° or 15°, the drag reduction can be much greater than that predicted by the slender-cowl theory since cowl angle is the dominant parameter. However, this relatively large decrease cannot compensate for the high drag of these cowls at full flow.

INTRODUCTION

The usual method of predicting the drag of an air-induction system through a range of engine operating conditions at a certain flight Mach number is to estimate the components of the net drag. (As shown in reference 1, net drag is a term consistent with the conventional definitions of net propulsive force and net thrust.) The net drag is the sum of the pressure drag on the cowl at full flow, the change in this force as mass flow is reduced, the scoop incremental or additive drag (depending on

whether or not a forebody interferes with the engine streamtube), and the skin friction. As discussed in reference 1, the net pressure drag in subsonic flight is zero if the flow is irrotational outside the boundary layer. Also, it was shown that, in supersonic flow, theory can reliably predict the pressure drag of isolated, symmetrical cowls with full flow for practical cowl angles and the additive drag of such cowls at the reduced mass-flow ratios encountered in normal flight. However, existing evidence shows discrepancies between theory and experiment and does not resolve the significant parameters for the change in cowl pressure drag with decreasing mass-flow ratio.

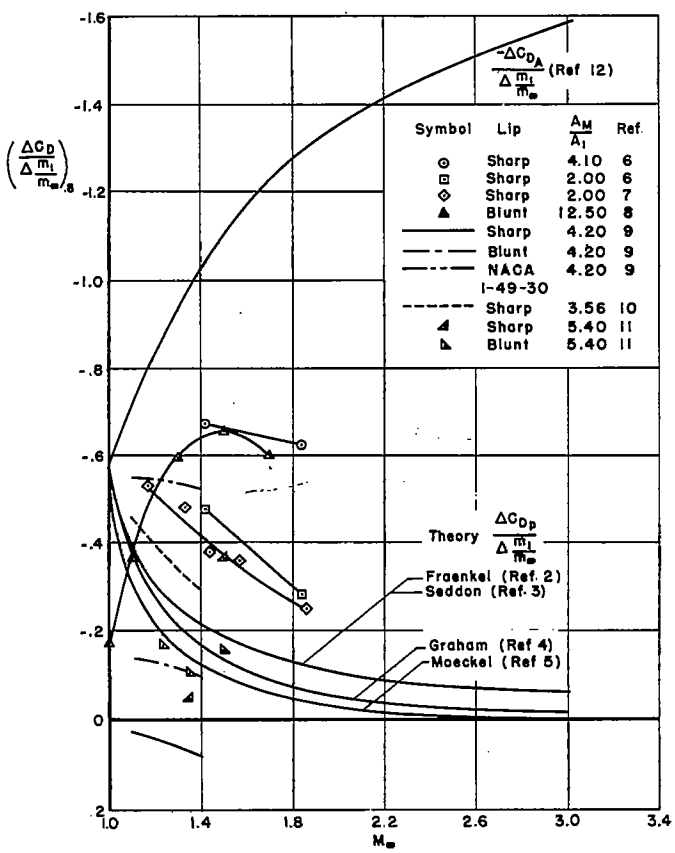

Theoretical methods for predicting the decrease in cowl pressure-drag coefficient with mass-flow ratio are presented in references 2 through 5. A summary of these theoretical results, together with experimental measurements (refs. 6 through 11) for comparison, is presented in the adjacent sketch. The ratio of the reduction in cowl pressure-drag coefficient to a decrease in mass-flow ratio from 1.0 to 0.8 $\left[\frac{\Delta C_{D_p}}{\Delta(m_1/m_\infty)}\right]_{0.8}$ is plotted as a function of flight Mach number. The corresponding increase in additive drag coefficient (ref. 12) $-\left[\frac{\Delta C_{D_A}}{\Delta(m_1/m_\infty)}\right]_{0.8}$ is also presented to illustrate the relative magnitude of the reduction in cowl pressure drag and to show that the additive drag is a dominating force even at low supersonic speeds. In compiling the information of this sketch, it was assumed that the variations of the cowl and additive drag coefficients, C_{D_p} and C_{D_A}, with mass-flow ratio were linear from mass-flow ratios of 1.0 to 0.8. In this range, the nonlinearity predicted by theory is small, particularly at Mach numbers greater than 1.4; in fact, the deviation from linearity is so small as to be within experimental accuracy.

In their theoretical predictions, Fraenkel and Seddon (refs. 2 and 3) use momentum methods and assume that the cowl is completely immersed in a subsonic flow field at stagnation conditions determined by the external normal shock wave. Seddon interprets his results by dividing the additive drag into two parts, wave and separation drag. The maximum separation drag is taken to be the local additive drag of the subsonic flow behind the normal shock wave, for this would be the net pressure drag of a thin-wall cylindrical tube in subsonic flow and would be the result of separation from the lips at reduced mass-flow ratios. The maximum wave drag is taken to be the difference of the over-all additive drag and this separation drag and is equal to the quantity that Fraenkel determines to be the sum of the additive drag and the change in cowl pressure drag from full flow. Thus, the ΔC_{D_p} of Fraenkel is equal to the negative of the maximum separation drag of Seddon. In comparing his method with experiment, Seddon adjusts the proportions of wave and separation drag according to cowl and lip shape to account for the fact that no consideration was given to effects originating downstream of the inlet plane in this subsonic flow field.

The theoretical prediction of Graham (ref. 4) and Moeckel (ref. 5) are for lip thicknesses which were chosen to produce the maximum suction force attainable according to the conditions assumed in the analyses. This optimum lip thickness is a function of flight Mach number. Also, it was assumed that a vacuum is maintained over the projected frontal area of the lip. Both of these investigations take the cowl to be simply a straight tube and consider the drag only to a fixed sonic point on the lip.

Comparison of the predictions with experimental results obtained by measuring pressure distributions on models with small cowl angles (refs. 6 and 7 where the ratio of maximum cowl frontal area to inlet area $A_M/A_1 = 2$) shows agreement as to the trend that the cowl pressure drag coefficient for a given change in mass-flow ratio decreases with increasing Mach number. However, the magnitude of the measured reduction in drag can be greater than predicted possible by Graham and Moeckel, particularly for the larger cowl angles (e.g., $A_M/A_1 = 4.10$). Fraenkel apparently overestimates the pressure which is attained downstream and thereby underestimates the possible suction force. Seddon adjusts according to the experimental conditions and finds that the drag of sharp thin lips is dominated by the separation drag at low supersonic speeds, but that the wave drag rapidly becomes more important as Mach number is increased. Also, the separation drag accounts for the nonlinearity of the variation of cowl pressure drag with mass-flow ratio, and this becomes important at low flow rates.

The data from tests in which only total forces were measured (refs. 8 through 11) show little consistency; this might be expected, for accurate measurements of the variation of a relatively small force are difficult to

obtain and also there is no assurance in such tests that the cowl pressure force is the only dependent variable. However, the data do suggest an effect of lip shape.

To clarify these discrepancies and to substantiate the trends indicated by theory, a series of pressure-distribution models of open-nose conical cowls were tested at Mach numbers from 1.3 to 1.9. The models had cowl angles of 5°, 10°, and 15°, and the 5° cowl was tested with four lip shapes, from a sharp to a relatively blunt leading edge.

SYMBOLS

A area, sq in.

C_D drag coefficient, based on inlet area, $\frac{\text{drag}}{q_\infty A_1}$

C_p pressure coefficient, $\frac{p - p_\infty}{q_\infty}$

d diameter of inlet, 2R, in.

L length of cowl to r_r, in.

m mass flow, slugs/sec

$\frac{m_1}{m_\infty}$ mass-flow ratio, $\frac{\rho_1 V_1 A_1}{\rho_\infty V_\infty A_1}$

M Mach number

p static pressure, lb/sq in.

p_t total pressure, lb/sq in.

q dynamic pressure, lb/sq in.

r radius, in.

R radius from model center line to center of lip radius r, in. (see fig. 2)

V velocity, ft/sec

x axial distance from lip leading edge, in.

y local lip ordinate, in.

Δ incremental value

θ cowl angle, deg

ρ mass density, slugs

Subscripts

∞ free-stream conditions

1 station at $x = 0$

1.0, 0.9, 0.8 mass-flow ratio at which drag measured

A additive

d dead-air region

L lip

M maximum

N net

p pressure

r reference radius of model, 1.5 in.

vac vacuum

APPARATUS

The tests were performed in the Ames 8- by 8-inch supersonic wind tunnel with the equipment described in reference 13. A photograph of the model mounted in the wind tunnel is shown in figure 1. The conical portion was removable so cowls with other lip shapes and cowl angles could be tested. The dimensions of these cowls and the locations of static-pressure orifices used to measure the pressure distributions are shown in figures 2 and 3. The mass flow through the duct was measured with a calibrated orifice meter.

The cowl models were chosen to provide information on the effects of cowl angle and of lip shape. Models 1, 2, and 3, and 6 all had a cowl

angle of 5° but different lip shapes and thicknesses. Model 1 had a sharp lip; model 2 had a lip with a semicircular profile; and models 3 and 6 had lips of elliptical profile, but of different thickness, with a ratio of major-to-minor axis length of 3.6 as recommended in reference 1. The lips of models 4 and 5 were elliptical with the same internal ordinates as model 3, but with cowl angles of 10° and 15°, respectively. The profile of the cowls was a straight taper, for, as shown in reference 1, this shape is very nearly that for minimum drag.

TEST PROCEDURE

The method of performing the tests was to set the desired Mach number and Reynolds number and to permit full flow through the duct. The flow rate was then reduced with measurements of mass flow and static-pressure distribution being taken. This procedure was repeated for different Mach numbers with total pressure adjusted to maintain essentially a constant Reynolds number. Because of wind-tunnel blockage, compressor, and support-interference limitations, the range of conditions at which reliable data were produced is as follows:

Models	Mach number
1, 2, and 3	1.34 - 1.88
4	1.41 - 1.88
5	1.51 - 1.88
6	1.41 - 1.88

The Reynolds number variation during the tests was from 2.34×10^6 to 2.56×10^6, based on a model reference diameter of 3.0 inches. All the tests were made at zero angle of attack and measurements were taken at mass-flow ratios from the maximum to about 0.7.

METHOD OF DATA REDUCTION

Although the main objective of the investigation was to determine only incremental effects of changes in model shape and flow conditions, it was considered desirable to estimate absolute values of the pressure and drag coefficients in order to obtain results comparable to other investigations. Thus, the data have been corrected for static-pressure gradients through the wind-tunnel test section. The necessary corrections were determined by comparing the measured distribution of the 5° cowl with a sharp lip (model 1) operating at full flow with the distribution calculated by the method of reference 14. This comparison is illustrated in figure 4. The comparisons at Mach numbers of 1.41 and 1.88

represent the greatest differences encountered in the tests; the data at 1.60 Mach number are typical of the other speeds. Since the theory is known to be reliable for sharp lips and small cowl angles, the differences in these distributions were used as corrections for the nonuniform flow conditions existing in the wind tunnel. The data taken at reduced mass-flow ratios and on other cowls were corrected by adding the differences for corresponding test conditions; thus, it has been assumed that the corrections are not significantly affected by the relatively small mass-flow and dimensional changes of these tests. Although the greatest differences represent large percentages of the local pressure level, as will be demonstrated later, these errors are of secondary significance in terms of the relative drag of several cowls tested at the same tunnel conditions or in terms of the variation of drag with mass-flow ratio of a given cowl. The reliability of the corrections is indicated by the consistency of the pressure distributions obtained.

As indicated in figure 4, the pressure distribution on long tapered cowls approaches as an asymptote the pressure coefficient of an equivalent cone. However, side interference affected the experimental data before the asymptote was very closely approached. The source of the interference was an expansion from the trailing edge of the mounting plate shown in figure 1. The data that were influenced by this expansion are shown in figure 4 by the symbols with arrows. The correction used for this expansion was the same as that for tunnel pressure gradient, that is, the difference between the theoretical prediction and the experimental data for a sharp-lip 5° cowl. Because of the large correction that is required at the downstream orifices, these data were not used in the integration of the pressure distributions to obtain drag coefficients. The maximum radius of the models was selected to be 1.5 inches, and the pressure data for all cowls were integrated to the corresponding axial station to obtain drag.

ACCURACY

The accuracy of the data was estimated by considering the magnitude of the corrections, the scatter from repeated runs, the manometer lag and reading error, and the root-mean-square uncertainty where multiple terms are involved in the calculation of a particular parameter. Estimates thus obtained are summarized in the following table:

Parameter	Uncertainty
p	±0.025 lb/sq in.
p_t	±0.025 lb/sq in.
M_∞	±0.01
m_1/m_∞	±0.4 percent relative uncertainty in a given run ±1 percent uncertainty in absolute value due to uncertainty in M_∞
C_p	±0.02
C_D	±0.002
$\frac{\Delta C_{D_p}}{\Delta(m_1/m_\infty)}$	±0.025

The maximum scatter of the experimental data is comparable to these estimated uncertainties except for the drag coefficient. For models 1, 2, 3, and 6, the maximum scatter of a few individual data points was ±0.0035 from a straight line drawn through the data for the variation of drag coefficient with mass-flow ratio. For models 4 and 5, this maximum scatter was ±0.01 because of the much larger drag coefficients. Thus, for drag coefficient, the usual uncertainty is as estimated, but in a few instances the errors were considerably greater. However, these occasional and inconsistent deviations from the general trend are not believed to be significant in affecting the main conclusions of the investigation.

To determine the stagnation pressure at an inlet lip, it was assumed that the stagnation streamline passed through a normal shock wave. In order to check this assumption, the stagnation pressure was measured for a range of mass-flow ratios by three different methods; these were (1) measurements were made with a total-pressure tube placed near the lip; (2) schlieren photographs were taken to determine the inclination of the external shock wave on the stagnation streamline; (3) the maximum pressure indicated by the leading-edge static-pressure orifices was recorded. The total pressures obtained from the assumption were in agreement with the measurements within the experimental accuracy.

RESULTS AND DISCUSSION

Pressure Distribution

Representative pressure-distribution data are presented in figures 5 through 8 in terms of pressure coefficient C_p as a function of the ratio of local frontal area to inlet area A/A_1. This independent variable is used because it spreads the data near the lip leading edge, and it is convenient because the areas between the curves and the abscissa are proportional to the pressure-drag coefficient. Values of A/A_1 less than

1 indicate surfaces inside the models. Data are presented for two Mach numbers, 1.51 and 1.88, and for a range of mass-flow ratios. The effects of lip shape and thickness are illustrated by a comparison of figures 5, 6, and 7, which show data for models 1, 3, and 6; the cowl angles are the same, 5°, but model 1 has a sharp leading edge, and models 3 and 6 have elliptical lips of different thickness. The effect of cowl angle is shown by comparing figures 6 and 8 which are for models 3 and 5; they have the same leading-edge shape but cowl angles of 5° and 15°.

Since the data have been corrected to agree with theory at full flow, for the sharp-lip cowl (fig. 5), the pressure coefficients at the leading edge approach those of a two-dimensional wedge of 5° semiapex angle, and downstream the coefficients approach those of a cone of 5° semiapex angle. For the reduced mass-flow ratios, the pressure coefficients immediately downstream of the leading edge have been assumed to be those predicted by the method of Chapman, Kuehn, and Larson (ref. 15) for dead-air regions caused by turbulent boundary-layer separation from a sharp edge, and the curves have been arbitrarily faired to these values. Actually, the boundary layer over the separation bubble is probably transitional (that is, transition occurs between the separation and the reattachment points), and, if this is the case, the pressure coefficients would be somewhat greater in magnitude. However, there is only a small change in the slope of the drag curve (i.e., $\Delta C_{D_p}/\Delta(m_1/m_\infty)$) if laminar separation is assumed, and the transitional separation would produce results somewhere between those for laminar and turbulent separation. It is seen that the minimum pressure coefficients predicted are about half of those corresponding to a vacuum at the leading edge.

For the rounded lips (figs. 6, 7, and 8) the maximum pressure coefficients measured indicate that the stagnation pressure on a lip is very nearly that existing behind a normal shock wave occurring at the free-stream Mach number. On the downstream portion of the cowl, the pressure coefficients are near the conical value at a distance somewhat greater than an inlet diameter. For all mass-flow ratios, the flow overexpanded immediately behind the leading edge and reached minimum pressure about where the straight taper of the cowl is tangent to the curved leading edge. The sonic point, as calculated from the assumption that the stagnation streamline passed through a normal shock wave, is in every instance between the first two external orifices, or very near the leading edge. The minimum pressure coefficients decrease with mass-flow ratio until the flow separates. Separation, as indicated by a region of constant pressure coefficient, apparently occurs at a mass-flow ratio of about 0.8 for the rounded lips tested with the 5° cowl angle. For the 10° and 15° cowls, separation occurs at lower mass-flow ratios, about 0.75. The prediction of the pressure in the separation bubble by the method of reference 15 is in good agreement with experiment for the thinnest lip of elliptical profile (model 3, fig. 6(b)) when turbulent separation is assumed. In fact, the prediction was in close agreement for both of the relatively sharp lips

(models 2[1] and 3), and the minimum pressure coefficients were about half of those corresponding to a vacuum. For the blunt lips (models 4,[1] 5, and 6), pressure coefficients from 60 to 75 percent of those for a vacuum were reached. These pressures on the blunter shapes might be expected because the minimum pressure coefficients attained on a circular cylinder with its axis normal to the flow are about three-quarters of those of a vacuum. (See ref. 16.) Downstream of the minimum-pressure station, the flow is recompressed abruptly by an oblique shock wave as shown by the typical schlieren photograph of figure 9. This shock wave, although very weak, occurs even at the maximum mass-flow ratios attained in the tests, as shown by the pressure distributions of figures 6(b), 7(b), and 8(b) at mass-flow ratios of about 0.99.

Change in Cowl Pressure Drag With Mass-Flow Ratio

Figure 10 shows the integrated cowl pressures in terms of drag coefficent C_{D_p} as a function of mass-flow ratio for some of the cowl shapes for which the pressure-distribution data were presented previously. It is evident that the experimental variation can be either greater or less than that predicted by theory, depending upon the cowl. Comparison is made only with Fraenkel's theory at one Mach number because there is the same lack of agreement at the other Mach numbers and with the other theories. Model 5, that with the 15° cowl angle, has six times the drag of the 5° cowl at full flow; on the other hand, it has five times the decrease in cowl pressure drag with a decrease in mass-flow ratio. Lip 6, which represents the thickest lip of the 5° angle cowls produces less drag than lip 3, although the difference is relatively small in comparison to the pressure drag of model 5. The data for models 3 and 6 are plotted to an expanded scale to show the linearity of the variation of cowl pressure drag with mass-flow ratio for the increment from 1.0 to 0.8.

Cowl Pressure Drag at a Given Mass-Flow Ratio

Figure 11 shows a comparison of the cowl pressure-drag coefficients at a mass-flow ratio of 0.95 for the Mach number range of the tests. This mass-flow ratio was chosen because the maximum mass-flow ratios for models with lips of varying bluntness were different for each model and not always equal to 1. As mentioned previously, to obtain drag, pressures were integrated to the longitudinal station at which the model radius was 1.5 inches; thus, these drag results show the effect of cowl angle for models of varying fineness ratio for which the maximum diameter is constant. The data show that the drag increases rapidly with cowl angle and that the effects of lip shape and thickness are relatively small. The theoretical

[1]Pressure-distribution data on models 2 and 4 are not presented because they do not demonstrate anything significant.

predictions shown on the figure are for sharp-lip cowls with full flow as determined from figure 11 of reference 1. It is seen that the agreement is fair even though the conditions are not exactly as assumed in the theory.

Change in Cowl Pressure Drag With Mass-Flow Ratio as a Function of Mach Number

Figure 12 shows the ratio of the reduction in cowl pressure-drag coefficient to a decrease in mass-flow ratio from 1.0 to 0.8 as a function of Mach number. The vertical lines through some of the points represent the range of possible slopes that could have been faired through the measured data. For points without vertical lines, the reliability of the data is ±0.025, as illustrated in the figure. It is seen that the trend predicted by the theories is substantiated; that is, the quantity $-\Delta C_{D_p}/\Delta(m_1/m_\infty)$ decreases with increasing Mach number. However, the reduction in drag due to the change in mass-flow ratio is greater than predicted. Rather surprisingly, and contrary to a statement in reference 1, page 65, the sharpest lip on the 5° cowl consistently has less drag at reduced mass flow than do the rounded lips which do not have any extensive separation over most of the range of test conditions covered by these data. This result is presumably caused by the facts that high pressures act on a smaller frontal area with the sharp lip and that separation distributes negative pressure coefficients over a greater frontal area than for the other shapes tested with the 5° cowl. The 10° and 15° cowls have a much greater drag reduction with decreasing mass-flow ratio than do any of the 5° shapes because, relative to the greater cowl pressures at full flow, a decrease in mass-flow ratio causes lower local pressures near the leading edge and distributes these low pressures over a greater frontal area.

The curves of figure 12 have been cross-plotted in figure 13, and comparisons are made with data from other investigations. The variations of $\left[\frac{\Delta C_{D_p}}{\Delta(m_1/m_\infty)}\right]_{0.8}$ with cowl angle at Mach numbers of 1.4 and 1.8 are shown. The strong influence of cowl angle is seen to be linear within the accuracy of the data. For the same decrease in mass-flow ratio, the sharp-lip profile has less pressure drag than the elliptical profile for all the cowl angles tested in this and the other investigations.

SIGNIFICANCE OF RESULTS

The data of this investigation show that cowl angle is the dominant parameter in determining the reduction in cowl pressure drag with a decrease in mass-flow ratio in supersonic flight. A relatively large cowl angle can provide a large decrease in drag as mass flow is reduced, but this decrease is gained at the expense of greater drag at full flow. To illustrate these conflicting trends in regard to net wave drag, which is the force of interest in determining performance, drag coefficients from the present investigation have been tabulated to show the effects of cowl angle, lip shape, mass-flow ratio, and Mach number.

$M_\infty = 1.4$							
Model	$(\Delta C_{D_p})_{0.9}$	$(\Delta C_{D_p})_{0.8}$	$(C_{D_A})_{0.9}$	$(C_{D_A})_{0.8}$	$(C_{D_p})_{1.0}$	$(C_{D_N})_{0.9}$	$(C_{D_N})_{0.8}$
1 (5° cowl sharp lip)	-0.033	-0.066	0.103	0.206	0.052	0.122	0.192
3 (5° cowl elliptical lip)	-.020	-.040	.103	.206	.070	.153	.236
4 (10° cowl)	-.053	-.106	.103	.206	.315	.365	.415
5 (15° cowl)	-.080	-.160	.103	.206	.60	.62	.65
$M_\infty = 1.8$							
1	-.018	-.036	.128	.256	.050	.160	.270
3	-.013	-.026	.128	.256	.082	.197	.312
4	-.040	-.080	.128	.256	.327	.415	.503
5	-.057	-.114	.128	.256	.546	.617	.688

In the tabulation of $(C_{D_p})_{1.0}$, it is assumed that there is a negligible change in cowl pressure drag resulting from a change in mass-flow ratio from the maximum to 0.95; the column thus contains values taken from figure 11. This assumption is justified by the relative magnitudes of the drag coefficients; that is, $(C_{D_p})_{1.0}$ is actually larger than $(C_{D_p})_{0.95}$, but the error is small in comparison to the magnitude of C_{D_A} in the case of the slender cowls, or in comparison to C_{D_p} for the blunt cowls. The quantity ΔC_{D_p} is the drag increment between a mass-flow ratio of 1.0 and either 0.9 or 0.8.

It is apparent from this table that for slender cowls (i.e., θ about 5°) ΔC_{D_p} can be a sizable portion of $(C_{D_p})_{1.0}$ but both are dominated by C_{D_A}. For blunt cowls, ΔC_{D_p} can counteract a sizable portion of C_{D_A}, but then both are dominated by $(C_{D_p})_{1.0}$. Thus, drag increases so fast with

both increasing cowl angle and external diffusion of the entering stream-tube that the decrease in cowl force with decreasing mass flow cannot counterbalance the former factors. A low net wave drag requires small cowl angles and small spillage. Figure 12 shows that this is particularly true at Mach numbers greater than about 2, for then ΔC_{D_p} for slender cowls is very small compared to C_{D_A}.

There is also a conflicting trend when cowl angle is considered in relation to the skin-friction drag. If the ratio of inlet to maximum frontal area is given, a reduction in cowl angle decreases the wave drag at full flow, but it also increases the wetted area and thus the skin friction. Figure 12 of reference 1 shows that for a skin-friction coefficient of 0.0025, the optimum cowl angles θ for ratios of inlet to maximum frontal area from 0 to 0.2 are from 3° to 4° for supersonic Mach numbers below 2. From the practical standpoint, such relatively small angles are the significant ones because they minimize the wave drag and still are large enough to permit the enclosure of required equipment in an airframe. For instance, to assume an extreme case, the compilation of aircraft dimensions of reference 1 (p. 53) shows that a small ratio of inlet area to fuselage maximum frontal area for supersonic fighters is about 1/8. If a fineness ratio of 3 is assumed between the inlet and maximum diameter stations, the equivalent cowl angle would be about 6°. For a more representative case of an area ratio of 1/6 and a fineness ratio of 4, the angle would be about 4°; or, for a fineness ratio of 5, it would be about 3°.

As regards lip shape, the tabulation shows that the net wave drag coefficients of the sharp lip are considerably less percentagewise than those of the elliptical lip both with full flow (30-percent difference) and with reduced flow (from 12- to 20-percent difference). However, as compared to the effect of cowl angle, the difference between lip shapes is small. At full flow, the increase in drag between the sharp and elliptical lips on the 5° cowl is equivalent to less than a $1/2^{\circ}$ increase in cowl angle at Mach numbers of 1.4 and 1.8. With reduced flow, this difference in the change in cowl pressure-drag coefficient (ΔC_{D_p}) due to lip shape is equivalent to a 2° increase in cowl angle at a Mach number of 1.4, and a 1° increase at a Mach number of 1.8. In practical design, lip shape is determined by compromises in performance through the whole range of flight conditions. For instance, the superiority of the sharp lip in drag at high flight speeds must be weighed against the thrust loss it produces at the high mass-flow ratios of take-off. If one assumes the typical airplane dimensions and drag coefficients of reference 1 (p. 53), the differences due to lip shape that were measured in this investigation are less than 2 percent of total airplane drag. This rather small advantage of the sharp lip at high speed could be overcome by the difference in pressure recovery in the static condition, for in reference 11, rounded, thin lips are shown to produce about a 5-percent greater pressure recovery than a

sharp lip. The drag in supersonic flight can be appreciably decreased by relatively small reductions in cowl angle even if a lip shape that is acceptable from low-speed considerations is used.

As mentioned previously, the accuracy of the drag coefficients obtained from this investigation was not of a very high order. However, the preceding compilation shows that a high degree of accuracy is not required in the determination of the decrease in cowl pressure drag with reduced mass-flow ratio. For example, this decrease for the elliptical lip shape was never greater than about 15 percent of the sum of the cowl pressure drag at full flow and the additive drag. Thus an error of 10 or even 20 percent in determining ΔC_{D_p} has only a few percent effect on the net pressure drag of the propulsion system. The errors in the estimation of other drag components of a complete airplane can easily overshadow this inaccuracy, for the net pressure drag of the propulsion system under normal flight conditions should be a minor portion of the total drag. Similarly, the method of Fraenkel is sufficiently accurate for engineering purposes to predict the quantity $\frac{\Delta C_{D_p}}{\Delta(m_1/m_\infty)}$ for slender cowls; that is, as shown by figure 13, there is no significant error if Fraenkel's prediction is used for cowl angles less than about 5°.

CONCLUSIONS

This investigation of the decrease in cowl pressure drag with a decrease in mass-flow ratio for open-nose inlets at Mach numbers from 1.3 to 1.9 has produced the following conclusions:

1. Cowl angle is a dominant parameter, for large reductions in cowl pressure drag can be achieved at reduced mass-flow ratio by changing the cowl angle from 5° to 15°. However, this decrease is more than offset by the increased drag at full flow with the greater cowl angles.

2. For slender cowls (i.e., cowl angles less than about 5°) the theory of Fraenkel, which does not account for lip shape (R.A.E. Rep. Aero. 2380), provides an adequate estimation of the effect of mass-flow ratio on cowl pressure drag.

3. For slender cowls, the reduction in cowl pressure drag with a decrease in mass-flow ratio becomes insignificant at flight Mach numbers greater than about 2.

Ames Aeronautical Laboratory
National Advisory Committee for Aeronautics
Moffett Field, Calif., Mar. 6, 1956

REFERENCES

1. Davis, Wallace F., and Scherrer, Richard: Aerodynamic Principles for the Design of Jet-Engine Induction Systems. NACA RM A55F16, 1956.

2. Fraenkel, L. E.: The External Drag of Some Pitot-Type Intakes at Supersonic Speeds: Part I. British R.A.E. TN No. Aero. 2380, June 1950.

3. Seddon, J.: Note on the Spillage Drag of Pitot-Type Air Intakes at Transonic Speeds. British R.A.E. TN No. Aero. 2315, Aug. 1954.

4. Graham, E. W.: Notes on the Drag of Scoops and Blunt Bodies. Rep. SM-13747, Douglas Aircraft Co., Inc., Santa Monica, Apr. 13, 1950.

5. Moeckel, W. E.: Estimation of Inlet Lip Forces at Subsonic and Supersonic Speeds. NACA TN 3457, 1955.

6. Fraenkel, L. E.: The External Drag of Some Pitot-Type Intakes at Supersonic Speeds: Part II. British R.A.E. Rep. No. Aero. 2422 June 1951.

7. Griggs, C. F., and Goldsmith, E. L.: Measurements of Spillage Drag on a Pitot Type Intake at Supersonic Speeds. British R.A.E. TN No. Aero. 2256, Aug. 1953.

8. Sears, Richard I., and Merlet, C. F.: Flight Determination of Drag and Pressure Recovery of a Nose Inlet of Parabolic Profile at Mach Numbers from 0.8 to 1.7. NACA RM L51E02, 1951.

9. Sears, R. I., Merlet, C. F., and Putland, L. W.: Flight Determination of Drag of Normal-Shock Nose Inlets With Various Cowling Profiles at Mach Numbers from 0.9 to 1.5. NACA RM L53I25a, 1953.

10. Howell, Robert R.: A Method for Designing Low-Drag Nose-Inlet-Body Combinations for Operation at Moderate Supersonic Speeds. NACA RM L54I01a, 1954.

11. Mossman, Emmet A., and Anderson, Warren E.: The Effect of Lip Shape on a Nose-Inlet Installation at Mach Numbers from 0 to 1.5 and a Method for Optimizing Engine-Inlet Combinations. NACA RM A54B08, 1954.

12. Sibulkin, Merwin: Theoretical and Experimental Investigation of Additive Drag. NACA RM E51B13, 1951.

13. Frazer, Alson C., and Anderson, Warren E.: Performance of a Normal-Shock Scoop Inlet With Boundary-Layer Control. NACA RM A53D29, 1953.

14. Van Dyke, Milton D.: Practical Calculation of Second-Order Supersonic Flow Past Non-Lifting Bodies of Revolution. NACA TN 2744, 1952.

15. Chapman, Dean R., Kuehn, Donald M., and Larson, Howard K.: Preliminary Report on a Study of Separated Flows in Supersonic and Subsonic Streams. NACA RM A55L14, 1956.

16. Gowen, Forrest E., and Perkins, Edward W.: Drag of Circular Cylinders for a Wide Range of Reynolds Numbers and Mach Numbers. NACA TN 2960, 1953. (Formerly NACA RM A52C20)

CONFIDENTIAL

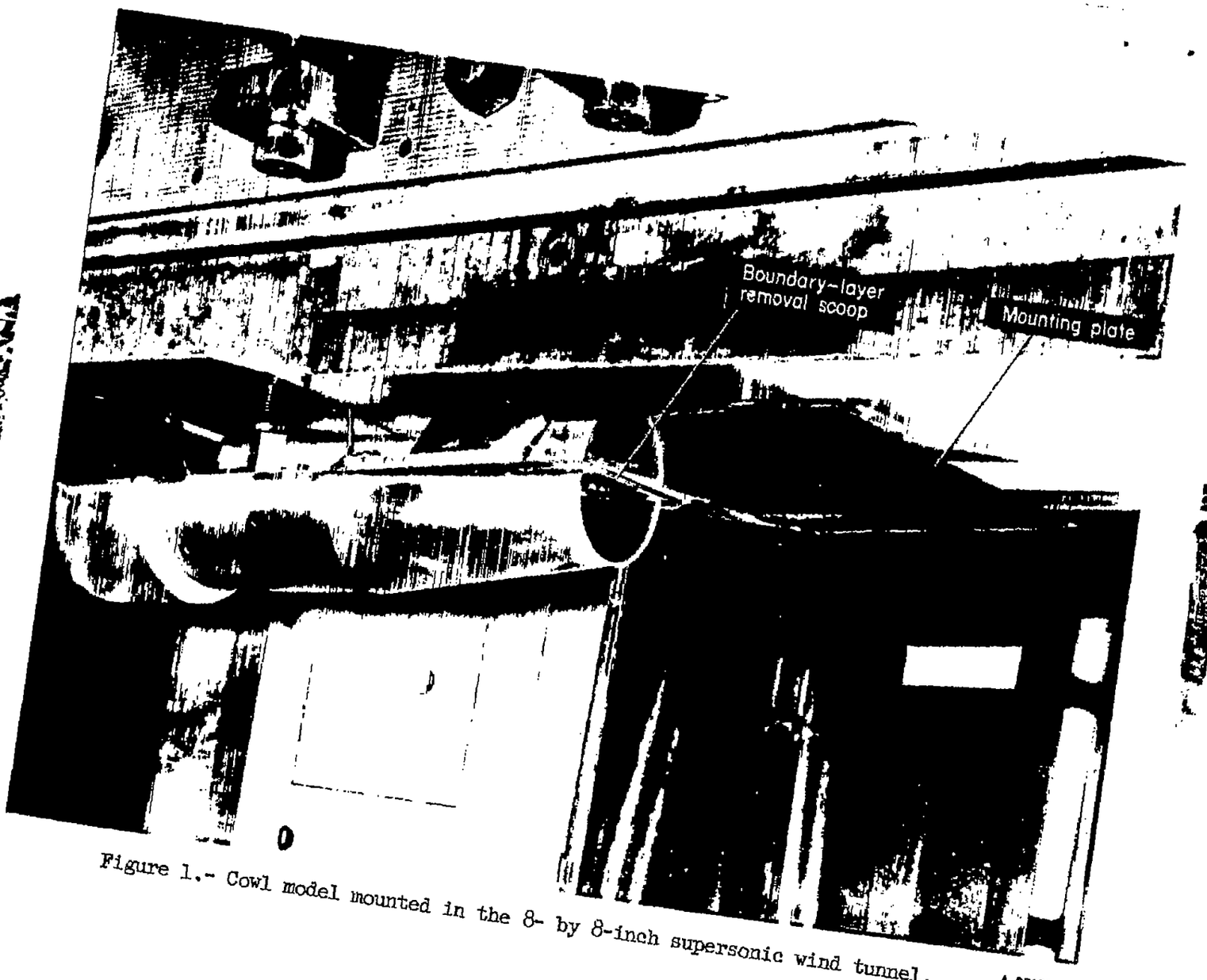

Figure 1.- Cowl model mounted in the 8- by 8-inch supersonic wind tunnel.

A-20131.1

CONFIDENTIAL

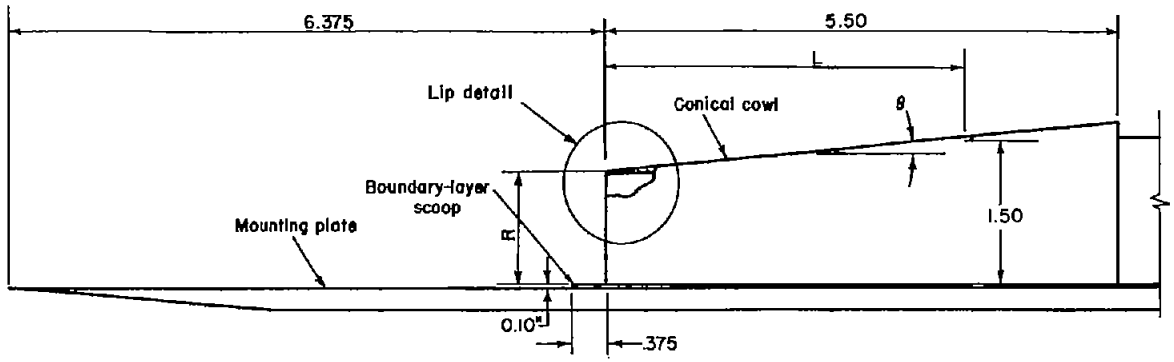

Model setup

Model 1

θ = 5°
R = 1.160
r = .001
L = 3.850

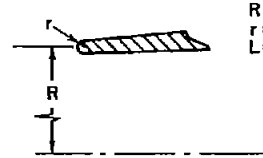

Model 2

θ = 5°
R = 1.148
r = .015
L = 3.385

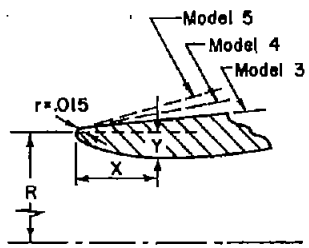

Model 3, 4 and 5

Model	θ	R	L
3	5°	1.189	3.160
4	10°	0.928	2.731
5	15°	0.925	2.094

X	Y
0	.002
.001	.005
.008	.014
.023	.025
.054	.037
.092	.046
.146	.053
.207	.056

All dimensions in inches

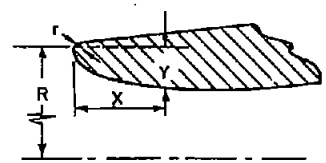

Model 6

θ = 5°
R = 1.246
r = .015
L = 3.875

X	Y
0	0
.018	.025
.056	.048
.100	.065
.148	.078
.246	.093
.350	.098

Figure 2.- Model dimensions.

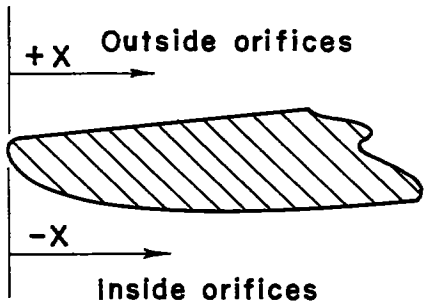

Orifice stations					
X inches					
Model 1	Model 2	Model 3	Model 4	Model 5	Model 6
.250	-.015	-.207	-.207	-.207	-.350
.500	-.009	-.100	-.100	-.100	-.260
1.000	-.001	-.050	-.050	-.050	-.170
1.500	.001	-.020	-.020	-.020	-.120
2.000	.009	-.007	-.007	-.007	-.080
3.000	.015	0	0	0	-.040
4.000	.063	.007	.007	.006	-.010
4.750	.125	.015	.015	.015	0
	.250	.063	.063	.063	.006
	.375	.125	.125	.125	.015
	.625	.250	.250	.250	.063
	.875	.375	.375	.375	.125
	1.500	.625	.625	.625	.250
	1.875	.875	.875	.875	.375
	2.375	1.500	1.375	1.375	.625
	2.875	1.875	1.875	1.875	.875
	3.375	2.375	2.375	2.375	1.375
	3.875	2.875	2.875	2.875	1.875
	4.375	3.375	3.325	3.000	2.375
		3.875	3.875		2.875
		4.375	4.375		3.325
					3.875
					4.375

Figure 3.- Orifice locations.

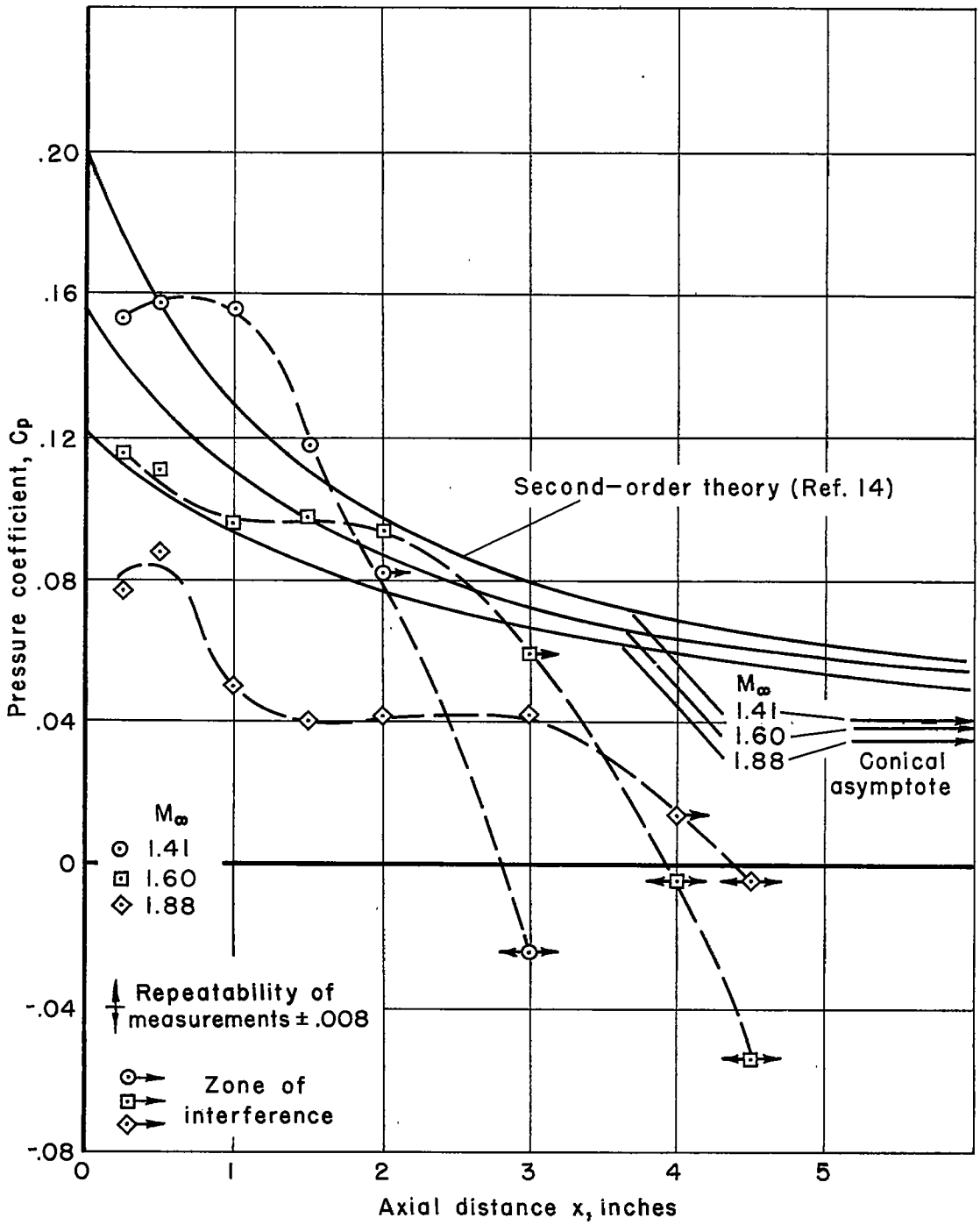

Figure 4.- Comparison of experimental and theoretical pressure distributions on 5° cowl with sharp lip and full flow.

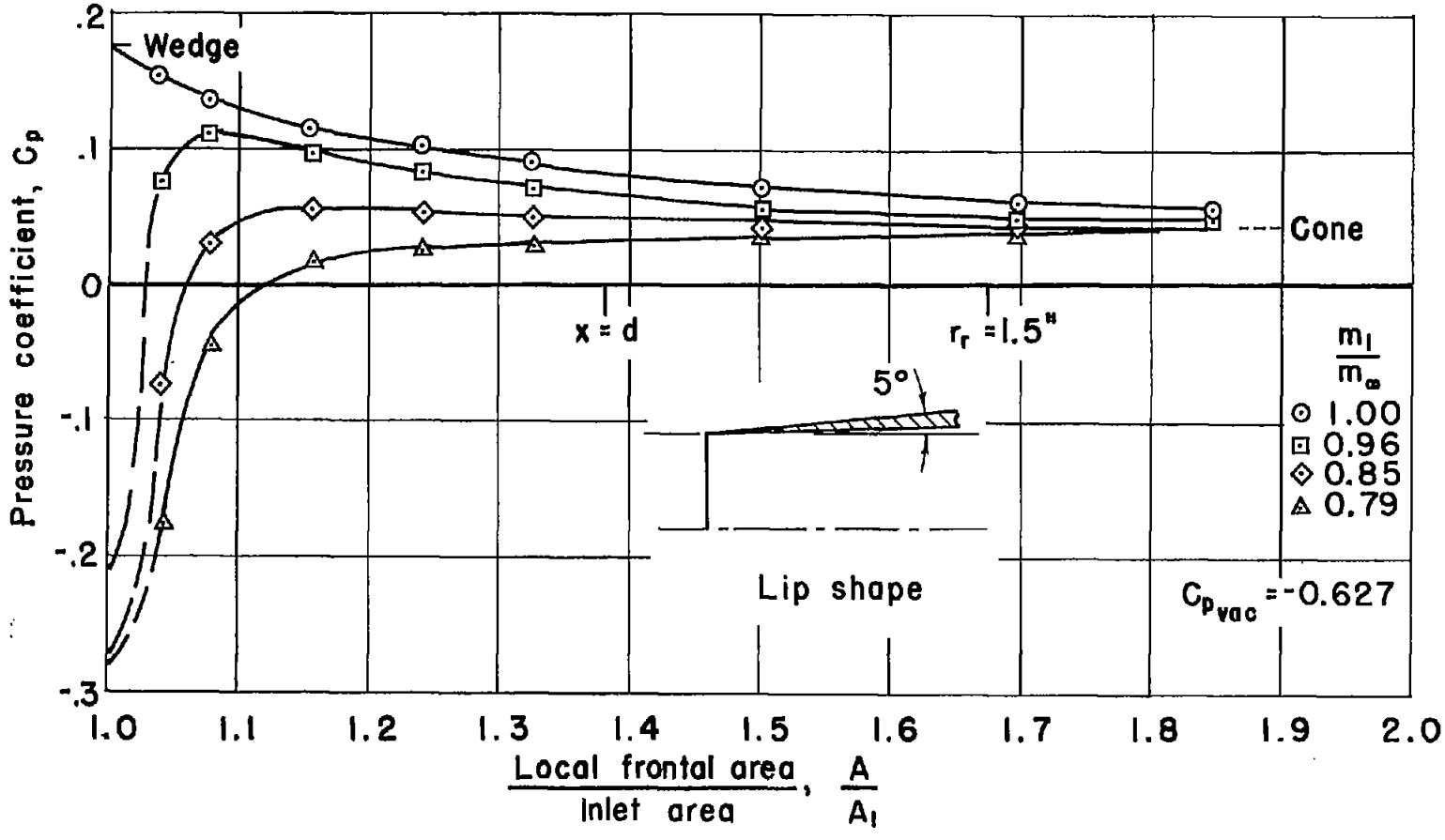

(a) M_∞ = 1.51

Figure 5.- Distribution of pressure coefficient on model 1.

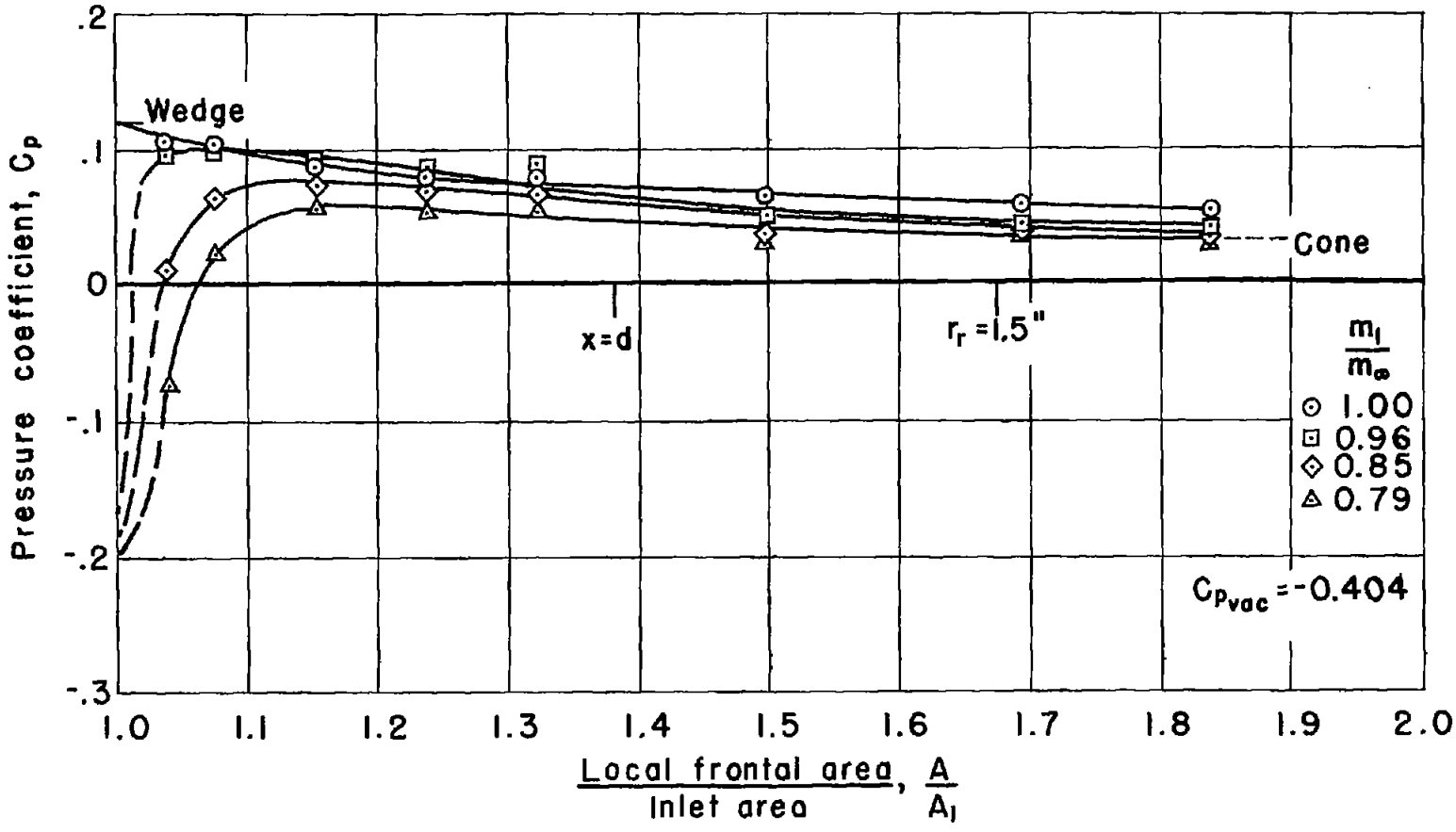

(b) M_∞ = 1.88

Figure 5.- Concluded.

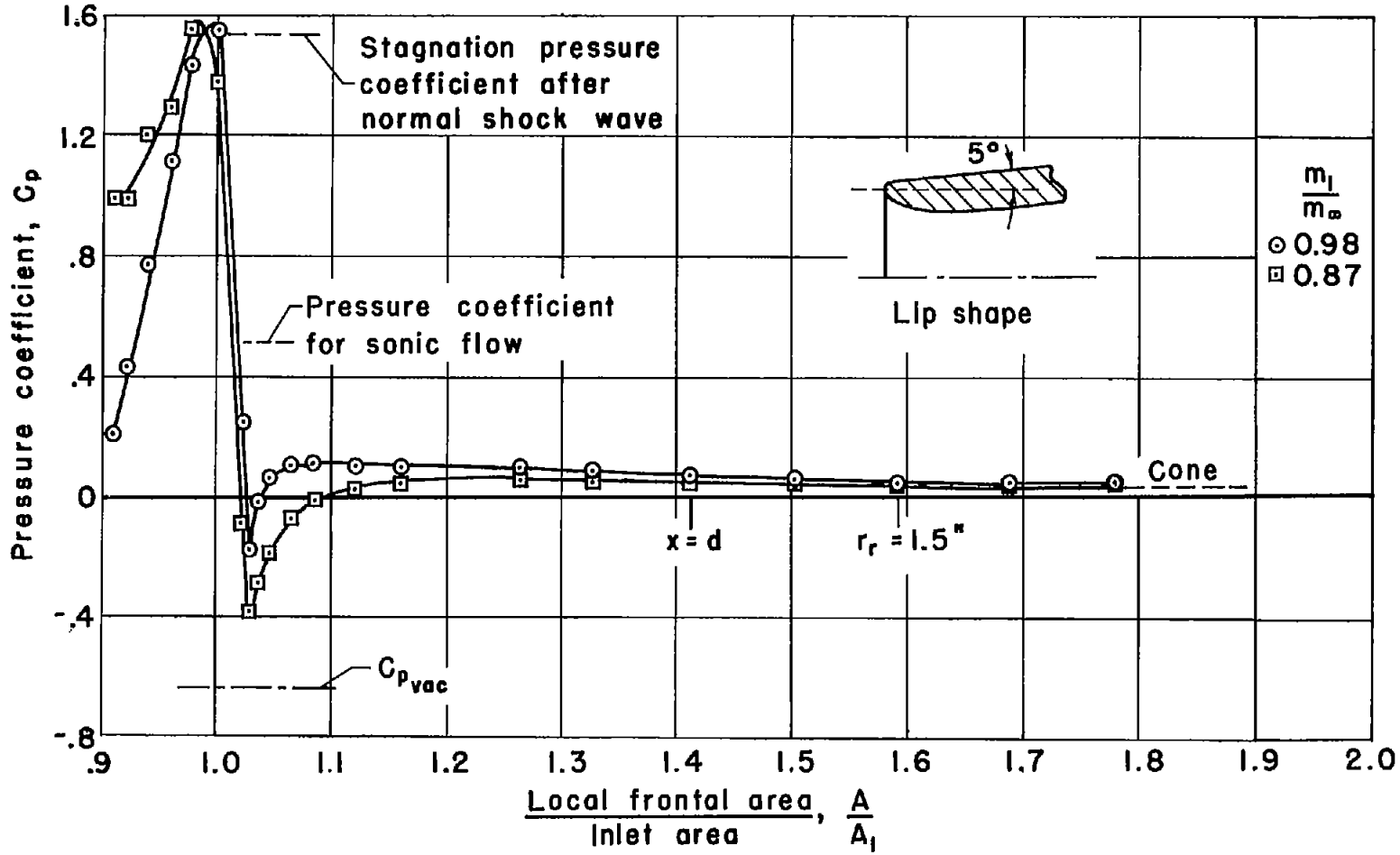

(a) $M_\infty = 1.51$

Figure 6.- Distribution of pressure coefficient on model 3.

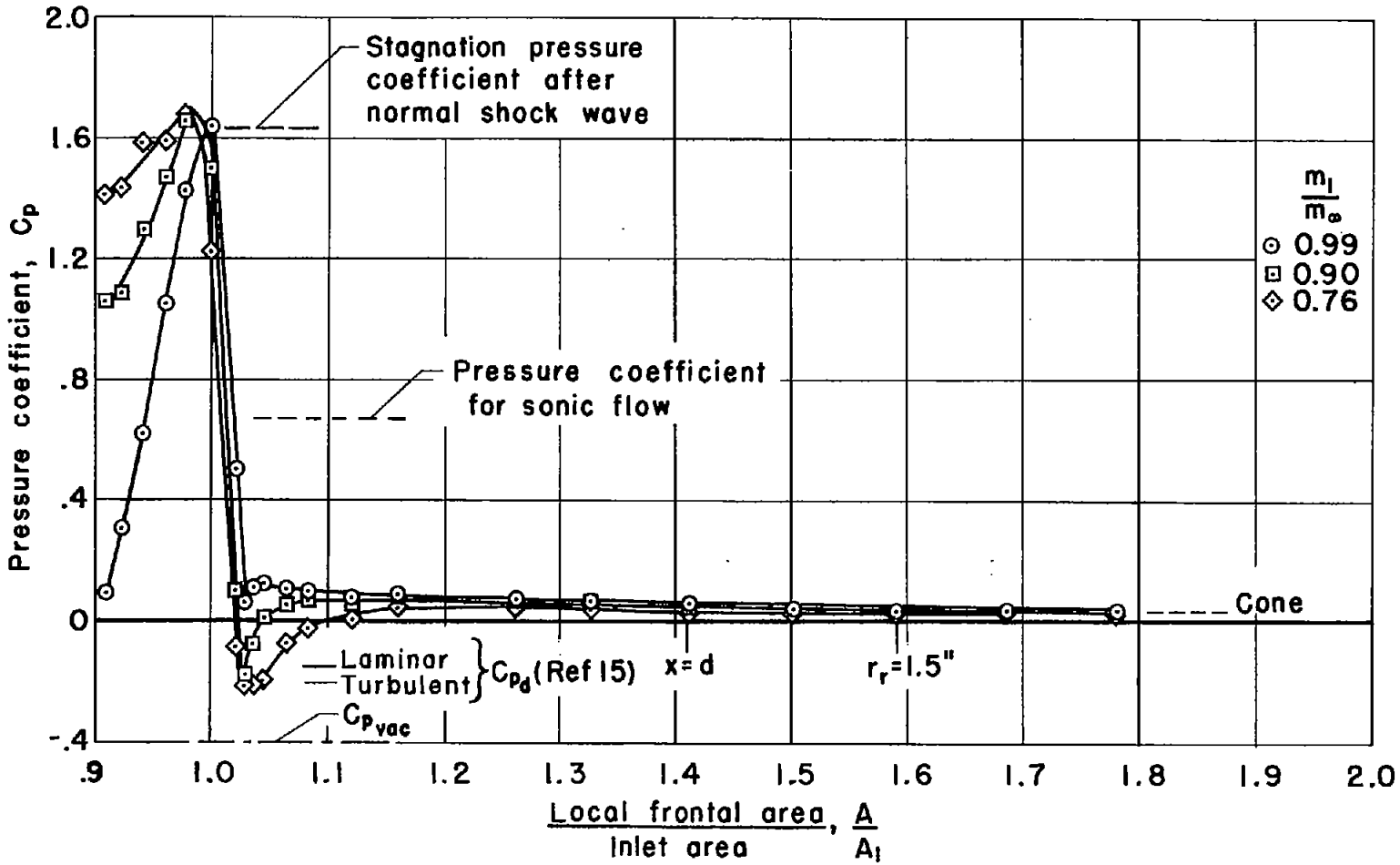

(b) $M_\infty = 1.88$

Figure 6.- Concluded.

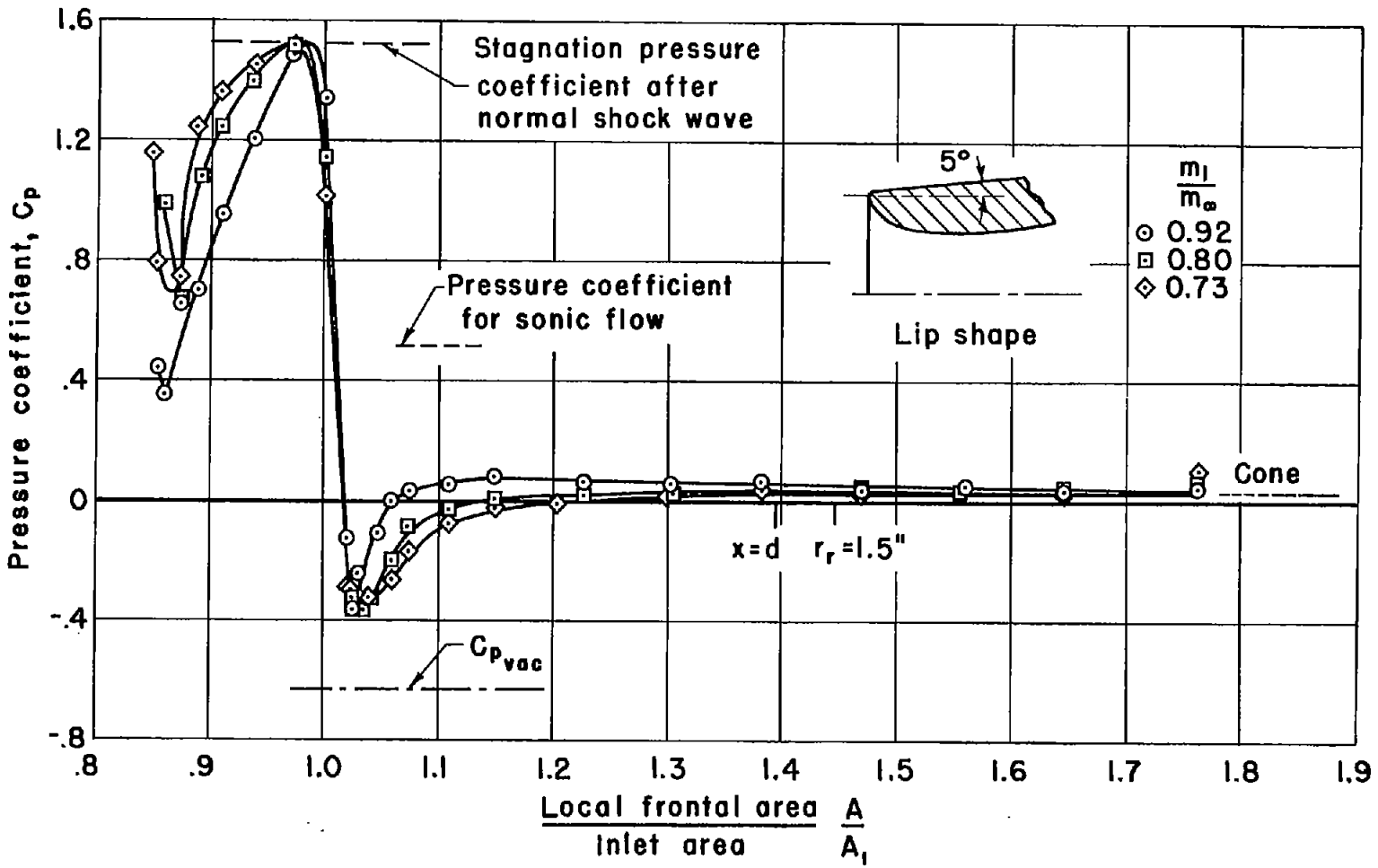

(a) $M_\infty = 1.51$

Figure 7.- Distribution of pressure coefficient on model 6.

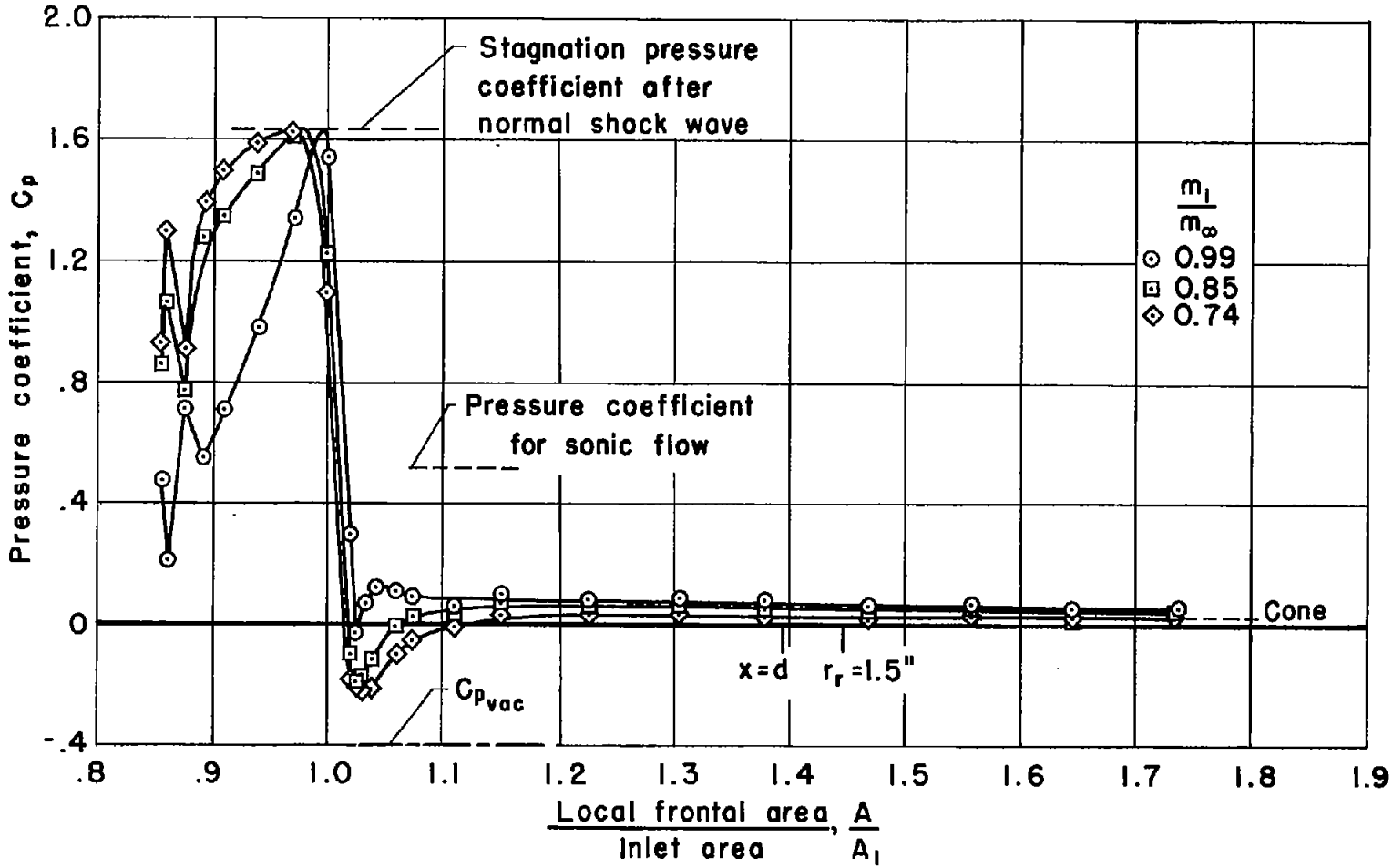

(b) $M_\infty = 1.88$

Figure 7.- Concluded.

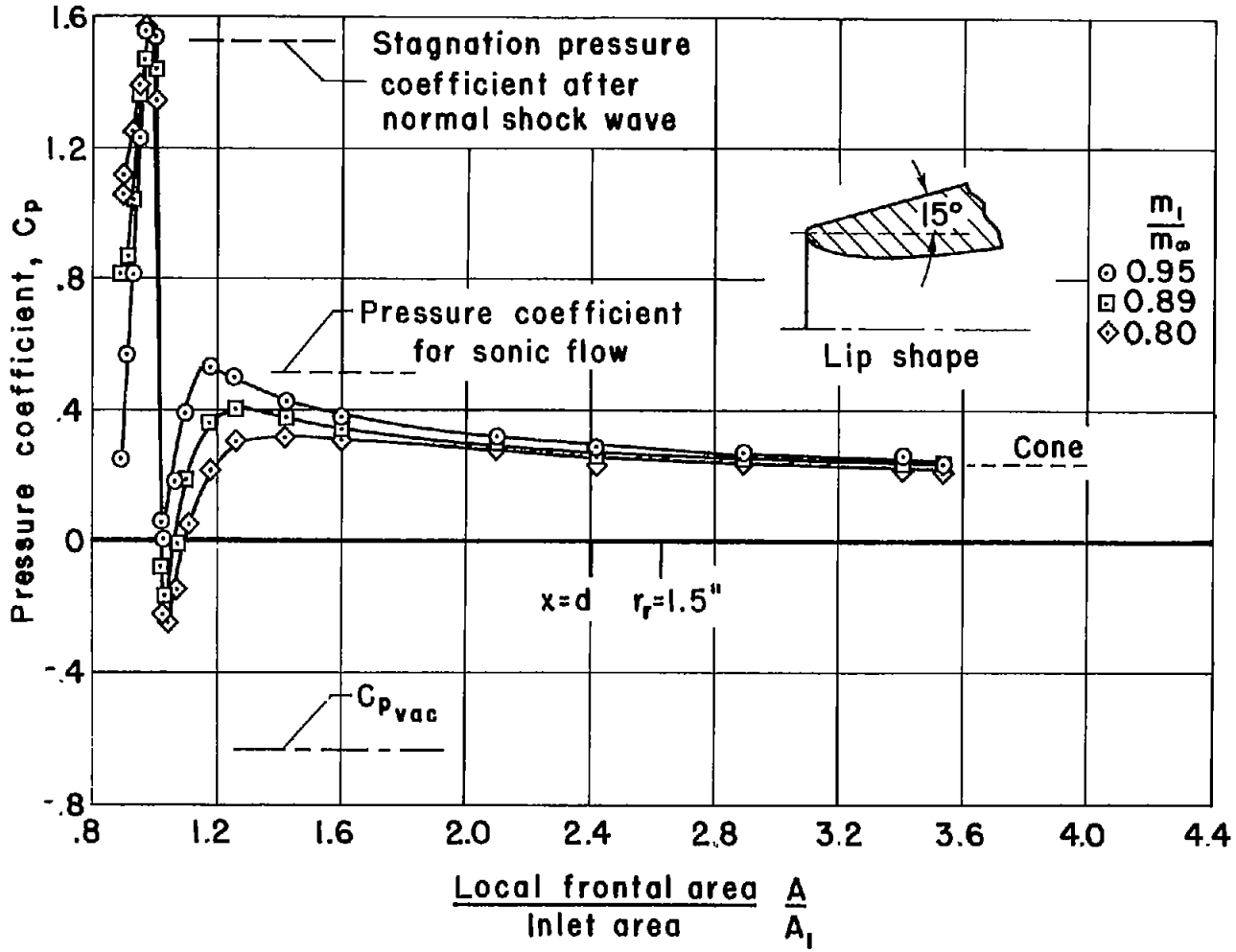

(a) M_∞ = 1.51

Figure 8.- Distribution of pressure coefficient on model 5.

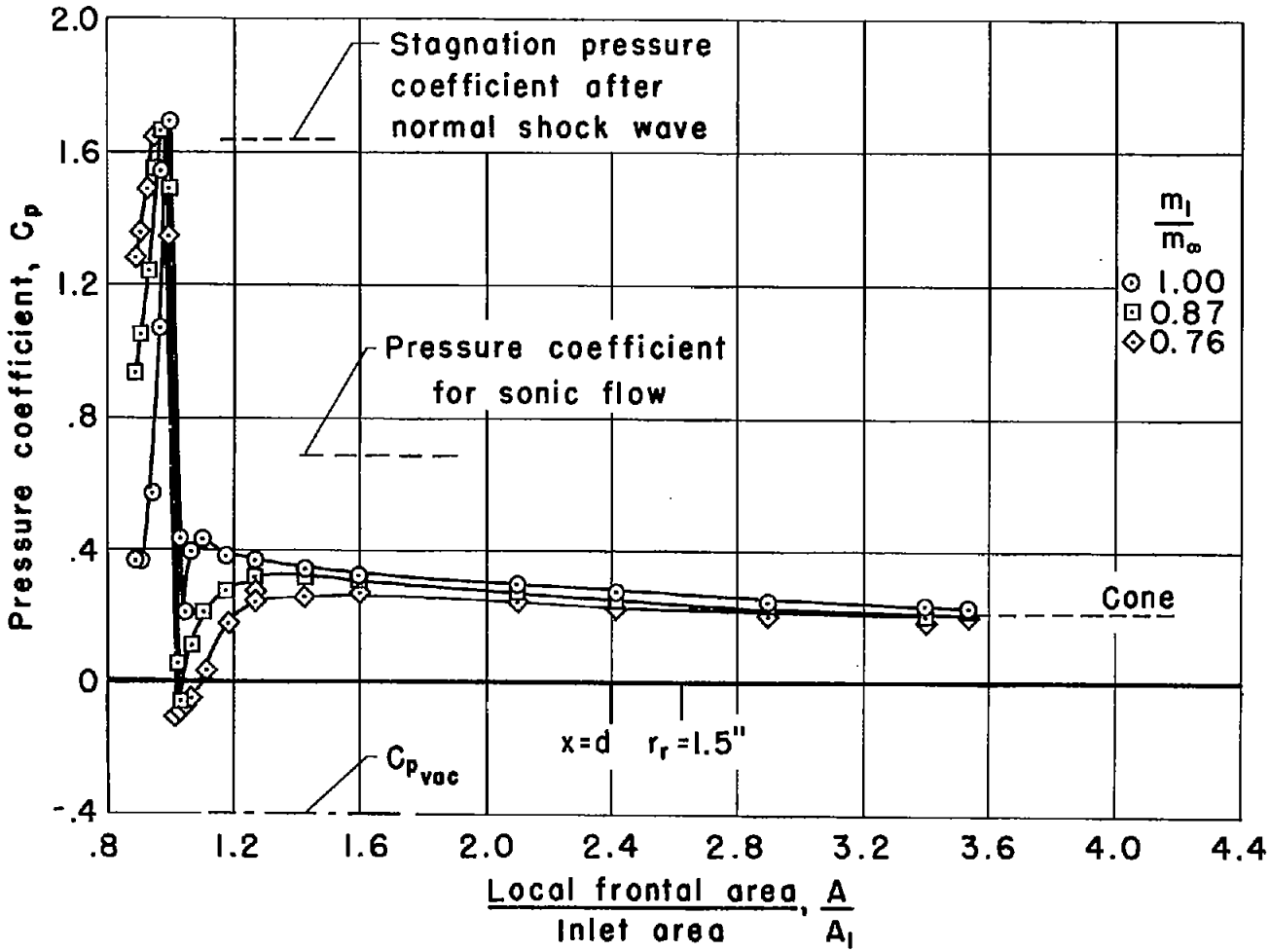

(b) M_∞ = 1.88

Figure 8.- Concluded.

UNCLASSIFIED

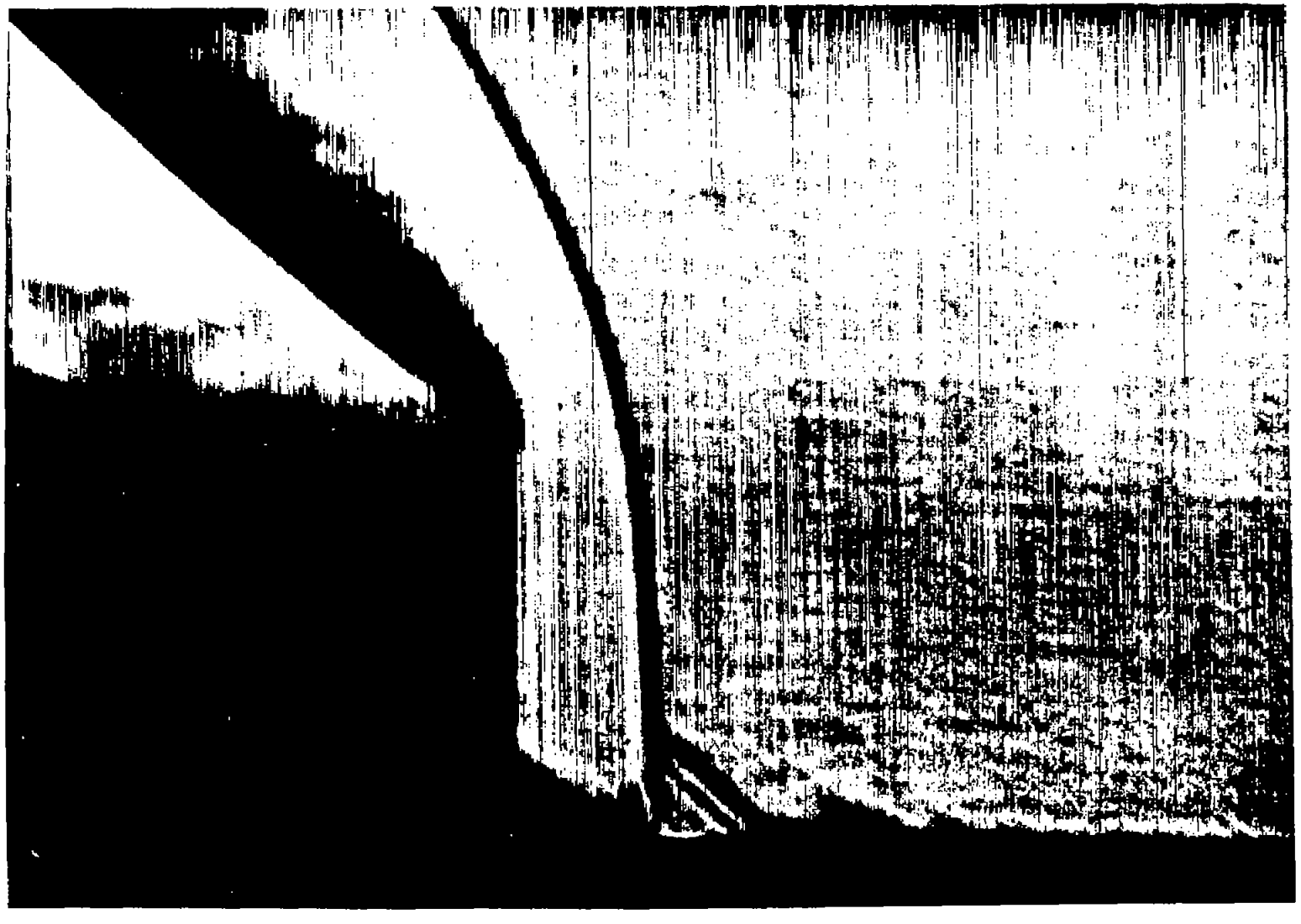

A-21176

Figure 9.- Schlieren photograph of model 3 ($M_\infty = 1.51$, $\frac{m_1}{m_\infty} = 0.87$).

UNCLASSIFIED

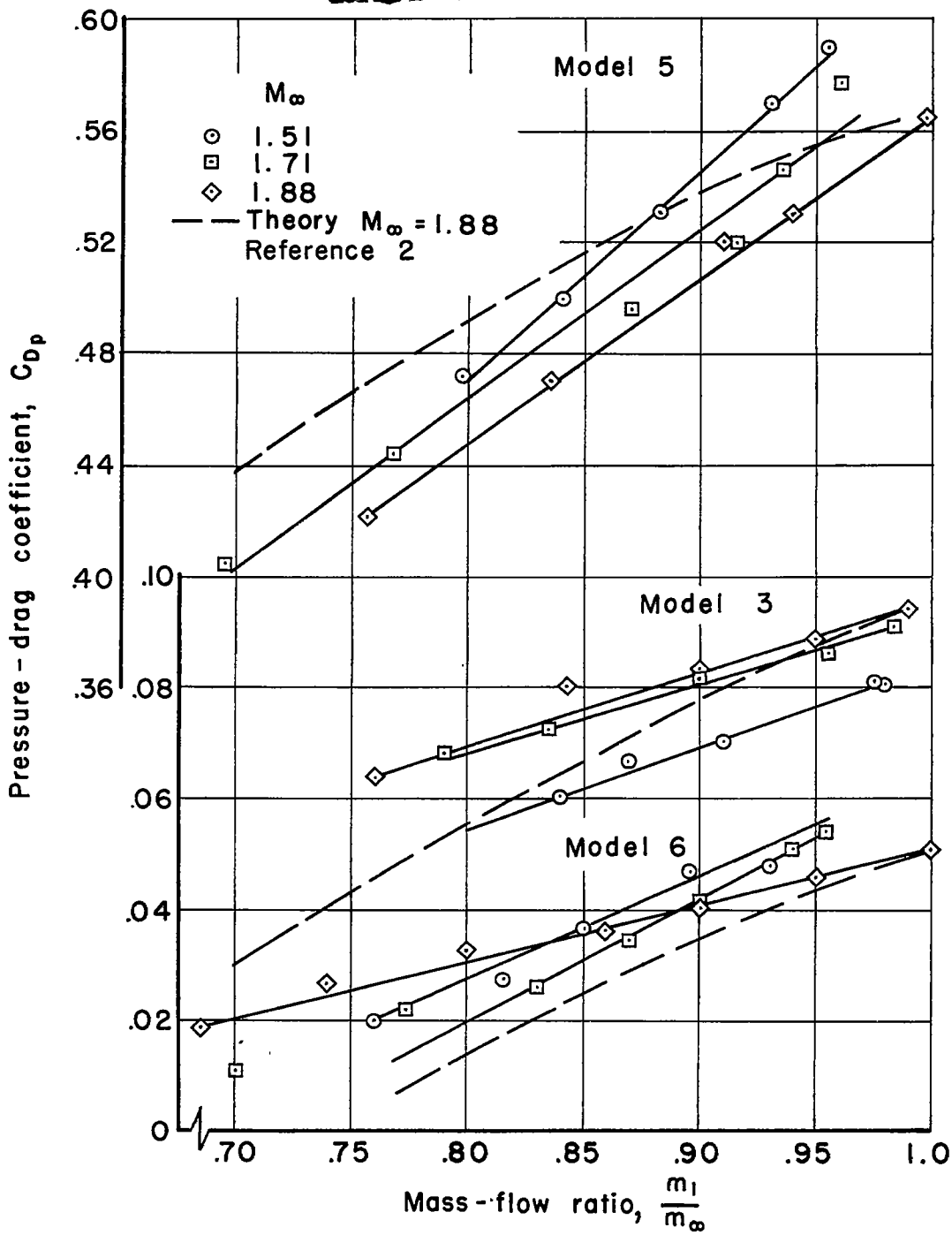

Figure 10.- Variation of pressure drag coefficient with mass-flow ratio for models 3, 5, and 6.

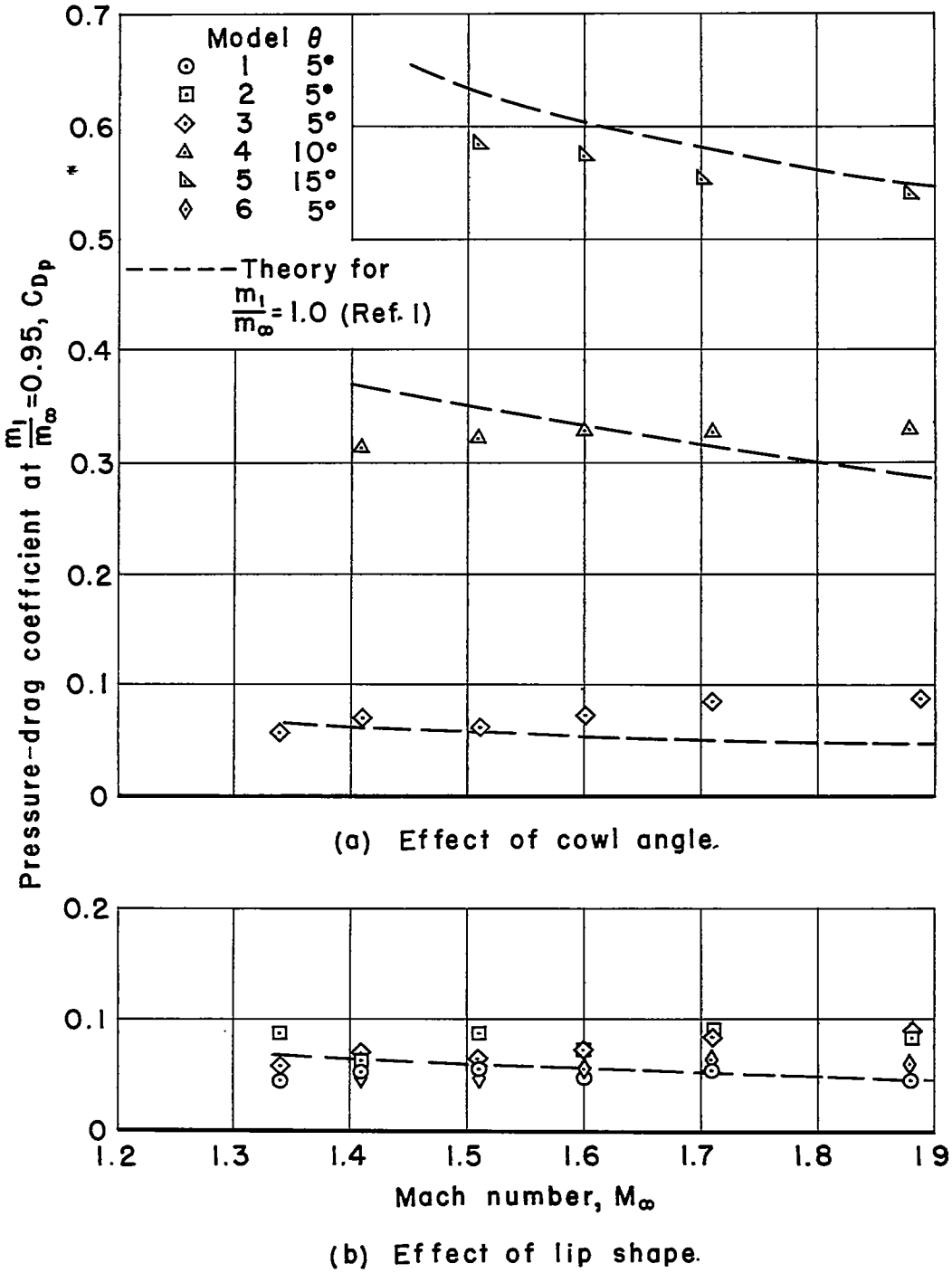

Figure 11.- Comparison of cowl pressure-drag coefficients at a mass-flow ratio of 0.95.

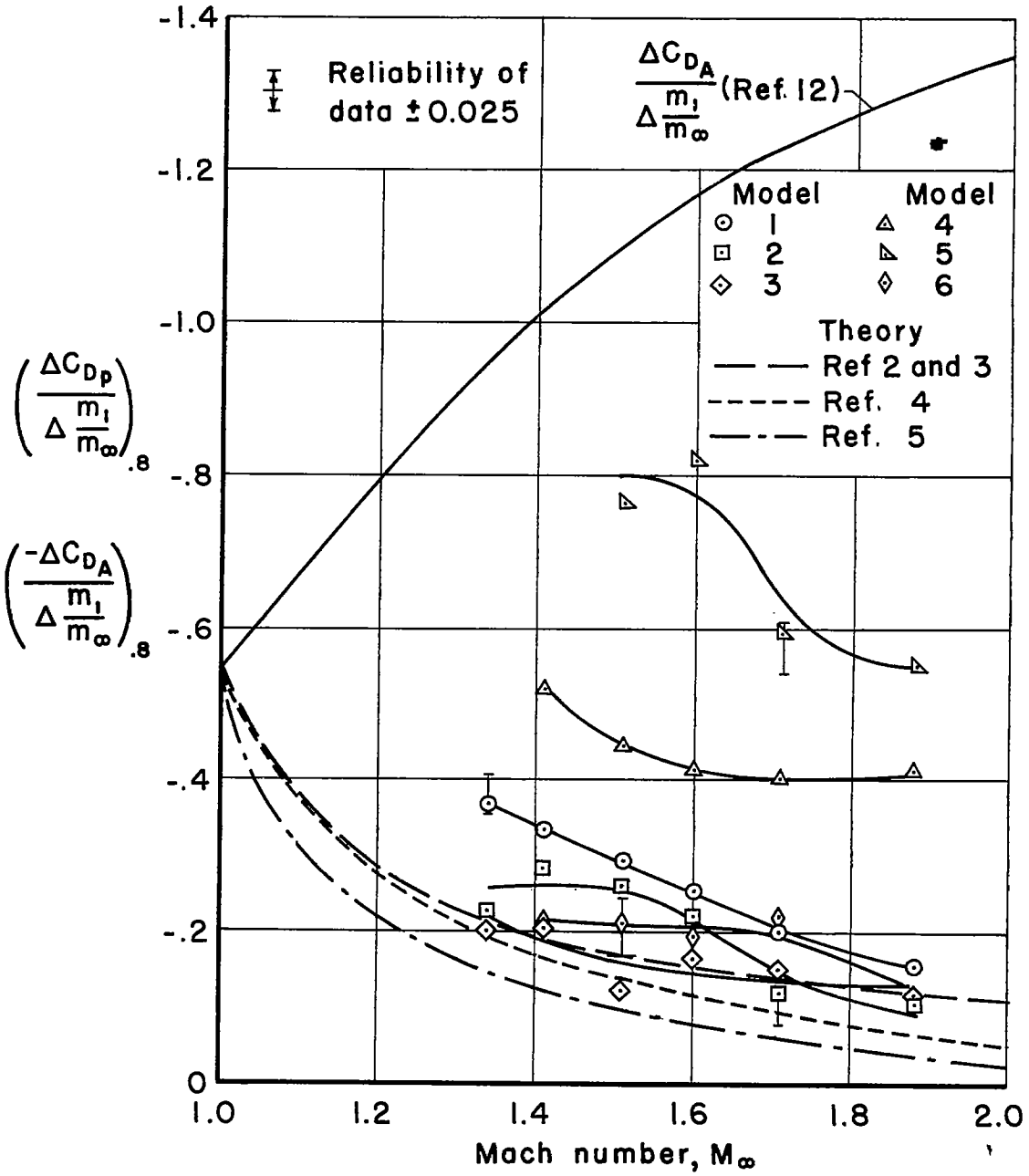

Figure 12.- The change in cowl drag coefficient with a change in mass-flow ratio as a function of flight Mach number.

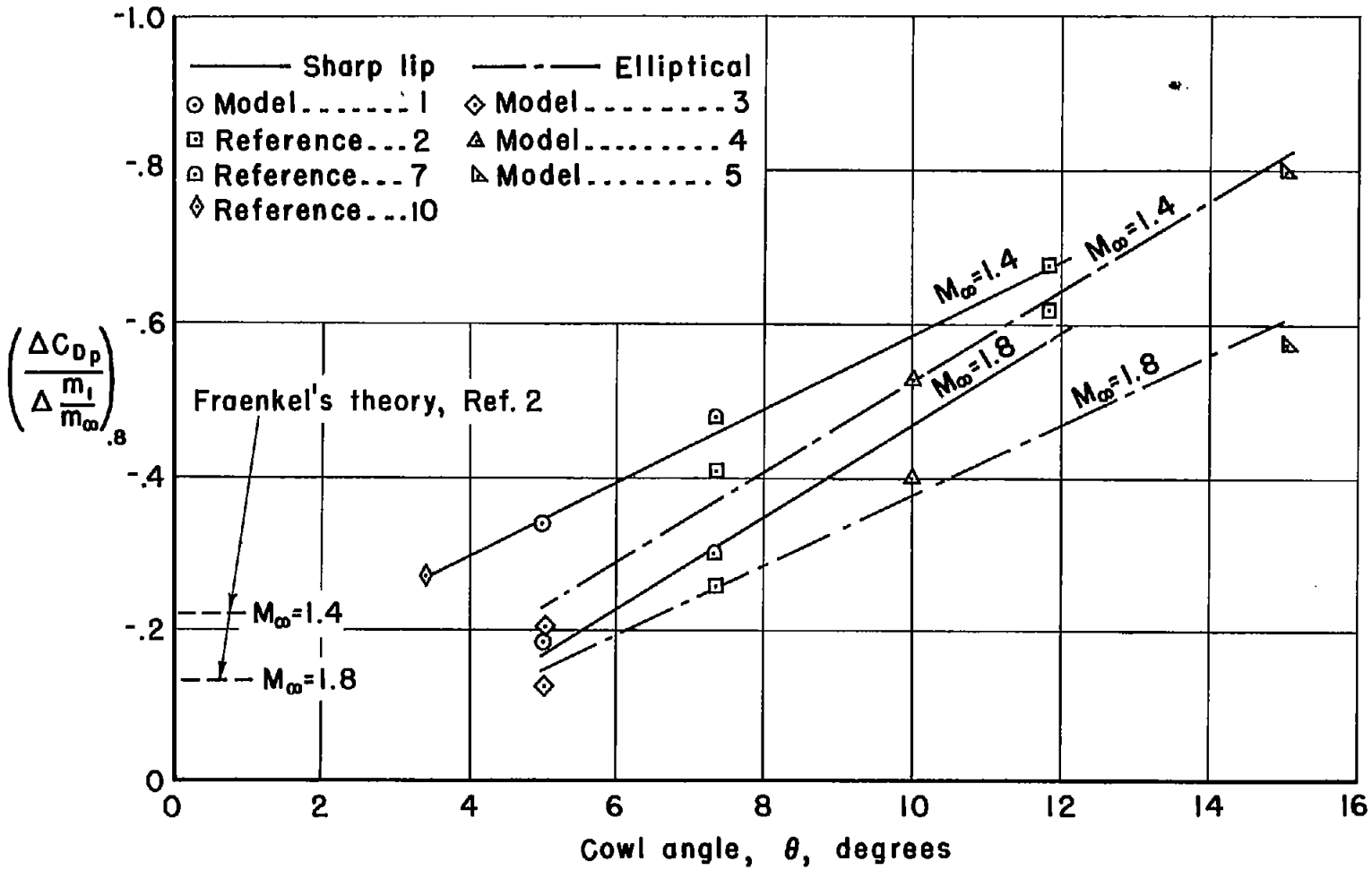

Figure 13.- Effect of cowl angle on the change in pressure drag with mass flow.

NACA - Langley Field, Va.